Effect of Placing High Voltage Direct Current on The Stability of Power System Generator Oscillation Damping Ratio

Ganiyu Adedayo Ajenikoko[1], Isaiah Gbadegeshin Adebayo[2] and Abass Balogun[3]
[1,2,3] Department of Electronic and Electrical Engineering, Ladoke Akintola University of Technology, Ogbomoso, Nigeria
Corresponding Email: ajeedollar@gmail.com
DOI:10.56201/ijemt.v10.no10.2024.pg53.70

Abstract

Application of Voltage Source Converter (VSC) such as High Voltage Direct Current (HVDC) has been widely recognized as one of the most advanced and powerful tools in providing a veritable way to control the transient instability in power system. However, the effect of this device on power system generator oscillation damping ratio during contingency need to be examined for effective system planning and monitoring. This research paper evaluates the effect of placing HVDC on the stability of power system generator oscillation damping ratio in order to improve the system stability during disturbance. Transient stability of electrical power system with contingency was performed using swing equations technique. Critical buses in the system at contingency was selected using Line-Voltage Stability Index (L-VSI) technique An HVDC VSC was incorporated in the power system and its effect on stability of the generator oscillation damping ratio at the contingency was investigated. Simulation was done in MATLAB R2023a. The approach was evaluated with data sets of IEEE 30-bus systems. Generator damping ratio, total active power losses and total cost of controllers were determined. The results revealed that placing HVDC in the power system improved the system generator oscillation damping ratio stability and has positive impact (stability) on electric power system

Keywords: *HVDC, Line-Voltage Stability Index, Voltage Source Converter, Contingency, Oscillation Damping Ratio*

1. INTRODUCTION

In developed countries, the annual consumption of electricity has been increasing rapidly while the expansion of transmission system has been severely limited due to inadequate resources Thus, power network has continuously been subjected to the greatest stress which has contributed to the constant power failure since greater demands have been placed on the transmission system by the continuous addition of load due to the increasing number of consumers [1, 2]. These disturbances adversely affect the transmission power expansion and cause instability in the transmission system, thereby becoming a major source of worry to engineers. Therefore, engineers have been faced with uphill tasks of designing power systems to optimally transmit energy at a

very stable state in which power systems can operate close to their thermal limits, either due to increased loading or due to severe contingencies [2 – 6] However, application of High Voltage Direct Current-Voltage Source Converter (HVDC-VSC) has been widely recognized as one of the most advanced and powerful tools in providing a veritable way to control the transient instability in power system during disturbance [1. 5. 7]

These HVDC-VSC devices employ self-commutated DC to AC converters, using Gate Turn-Off (GTO) thyristors, which can internally generate capacitive and inductive reactive power for transmission line compensation, without the use of capacitor or reactor banks. It provides unprecedented levels of flexibility and speed of response in comparison with traditional electromechanical devices [8 -11]. Thus, use of HVDC-VSC in transmission system is becoming more and more popular due to its wide range of advantages in bulk power transfer and integration of renewable power to the existing grid, Its importance has increased due to the increased awareness of energy conservation and quality of supply on the part of the power utility as well as power consumers [12-16]

However, improper placement of HVDC-VSC in electrical power system may increase the system instability, generator oscillation and thwarting the power system expansion planning [13, 17]. Therefore, there is the need to investigate the effect of proper placement of HVDC on the power system oscillation damping ratio. This is very much useful for power system monitoring and expansion to prevent possible voltage instability and to meet the increasing loads.

It is based on the foregoing that this study evaluates the effect of placing HVDC-VSC on the stability of electrical power system generator oscillation damping ratio during disturbance using Line-Voltage Stability Index (L-VSI) to identify critical buses for its placement.

A. Voltage Source Converter

The Voltage Source Converter (VSC) group FACTS device is the most advanced type among the FACTS controllers, employs self-commutated DC to AC converters, using Gate Turn-Off (GTO) thyristors, which can internally generate capacitive and inductive reactive power for transmission line compensation, without the use of capacitor or reactor banks. It can supply required reactive current even at low values of the bus voltage and can be designed to have in built short term overload capability. The converter with energy storage device can also exchange real power with the system [3, 14, 18].

The VSC devices include Static Synchronous Series Compensator (SSSC), Static Synchronous Compensator (STATCOM) and High Voltage Direct Current (HVDC) VSC device which is the focus of this research paper..

B. High Voltage Direct Current Based VSC

The High Voltage Direct Current based on Voltage Source Converters (VSC) is a combined series-series FACTS device which is controlled in a coordinated manner in a multiline transmission system [19, 20]. The controllability of the HVDC power is often used to improve the operating conditions of the AC network where the converter stations are located. The HVDC allows more efficient bulk power transfer over distances and it employed to move large amounts of electric power. The fundamental process that occurs in an HVDC system is the conversion of electrical current from AC to DC (rectifier) at the transmitting end and from DC to AC (inverter) at the receiving end. In this system, it is possible to control both active and reactive power

separately by exploiting Pulse Width Modulation (PWM) to control the On and Off time in the VSC. This technology does not consume reactive power, but rather, it injects reactive power to the power system [21-25].

In addition, HVDC VSC systems do not only allow for electrical power transmission from one area to another, it also offer several technical advantages. It offers technical and economic benefits, such as: lower line costs, no need for common frequency control, stable operation even with low-power interconnection and improved dynamic conditions in AC system [26]. However, in order to assess the maximum transfer capability of these devices on the power transmission system, its effect on system oscillation damping ratio which may have undesired effect on the power system stability be evaluated [27 -30].

I. MATERIALS AND METHOD

This study presented multi-objective optimization problems for improvement of power system generator oscillation damping ratio stability during sudden increase in generator load for efficient power system monitoring and planning. The main objective is to optimize the generator load bus with the least value of damping ratio that would improve the voltage stability of the power system. The multi-objective optimization problems are formulated as single objective function as Equation (1):

$$OF = Optimize \sum_{\substack{i=1 \\ j\neq 1}}^{N} \left(\Delta P_{GLi} + j \frac{\delta}{\partial t} K_D \right) \quad (1)$$

Subjected to stability constraint: damping ratio limit as in Equation (2):

$$0.03 \leq K_D \leq 0.05 \quad (2)$$

where; P_{GLi} is the equivalent generator power obtained at each load bus, K_D is the generator damping ratio coefficient, δ is the rotor angle, θ is the phase angle,

A. Data Source

The implementation of HVDC VSC was done on standard IEEE 30-bus power system shown in Figure 1. The test system has two (2) generators, three (3) synchronous condensers, 15 load buses (PQ). Out of the generator buses, bus 1 is selected as the slack bus [23]. The set of data such as line data, load data, generators and other system components data were sourced from the Institute of Electrical and Electronics Engineers (IEEE) website (http/ewh.ieee.org/soc/pes/tesl). The HVDC parameters were sourced from published open access literatures on the concept. The simulation was done under contingency analysis. In this case; the reactive power of the generator load power of the transmission system was adjusted from 50 to 90 % (20%b interval) one at a time. The minimum and maximum damping ratio were set to 0.03 and 0.05. Simulation wias carried out in MATLAB R (2023a). The change in the generator damping ratio were calculated. The system generator damping ratio, generator voltage, losses and cost of controller placement were determined in each of the test system and were used as performance metrics.

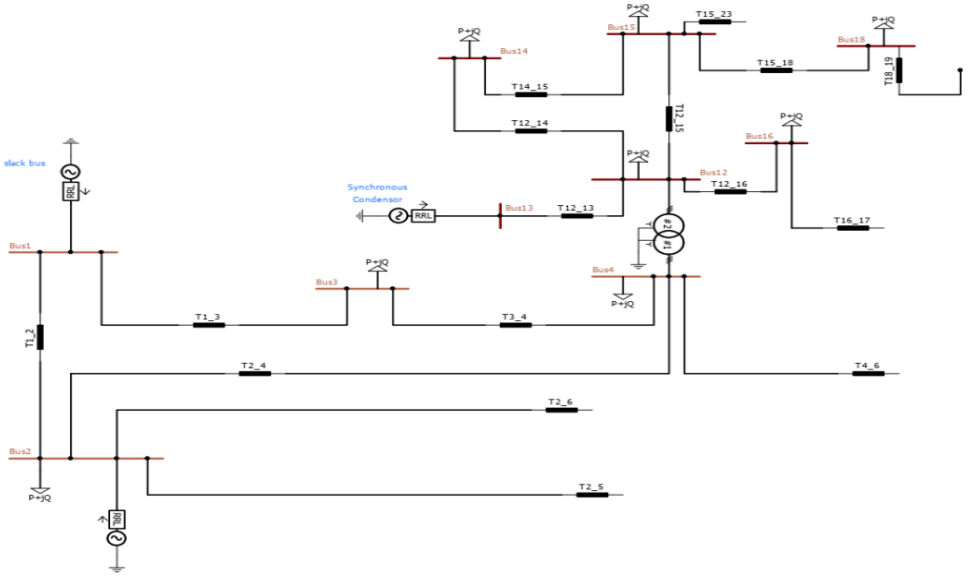

Figure 1: IEEE 30-Bus Test System

B. Transients Stability Analysis for Contingency

The power system generator oscillation damping ratio for transient stability of the transmission system was computed by adjusting the generator load power from 50 to 90 % one at a time and swing equation was employed. The minimum and maximum damping ratio was set to 0.03 and 0.05. Swing equation was analysed on the transmission system to obtain the dynamic behavior of the system generator oscillation during the increase in the generator load power. The system generator oscillation damping ratio was monitored for any bus close to the rating limit. The generator voltage, electrical and mechanical power were calculated using Equations (3) to (5) [4, 9]

$$E = V + jX_S\left[\frac{P_g - jQ_g}{V_i^*}\right] \tag{3}$$

$$P_{ei} = E_i^2 Y_{ii}\cos\theta_{ii} + \sum_{\substack{i=1 \\ j\neq 1}}^{N}\left|E_i\right|\left|E_j\right|\left|Y_{ij}\right|\cos\left(\theta_{ij} - \delta_i + \delta_j\right) \tag{4}$$

$$P_e = P_m - P_a \tag{5}$$

The behavior of the generator is given as in Equation (6) [2, 8]:

$$\frac{H\partial^2\Delta\delta}{\omega\cdot\partial t^2} = \Delta P_m - \Delta P_e \tag{6}$$

The generator damping ratio was calculated using Equation (7) [23, 30]:

$$\Delta K_{GDi} = \int_{0.03}^{0.05}\left(\Delta P_{GL} - \left|\Delta P_{ei} + \frac{H\partial^2\Delta\delta}{\omega\partial t^2}\right|\right)\partial t \tag{7}$$

C. Identification of Critical Buses

The Line- Voltage Stability index (L-VSI) was formulated to identify critical buses in the power system as to determine the best placement of the HVDC in the power system. This L-VSI was used to identify the critical buses, determine the optimal severity order of the load buses for optimum location of the HVDC-VSC in electrical power system.

The L-VSI was formulated using the weighted sum of normalized value of the system line loss and generator bus voltage based on the damping ratio s given in Equations (8):

$$L-VSI = \sum_{i=1}^{N}\left[w_1 \sum\left(\frac{Y_G X_S}{V_i^2} \right) + w_2 \sum\left(\frac{P_{Li} X_S}{V_i^2} + jQ_{Li} \right) + \Delta K_{Di} \right] \quad (8)$$

The load bus with highest value of L-VSI based on the fitness function was regarded as weak bus for potential placement of generator and VSC devices in power system,

where; $P_{L\,i} and\ Q_{Li}$ are active and reactive power loss, X_S is the system reactance, V_i is the system internal voltage, Y_G is the element of generator bus admittance matrix, w_1 is the weighted coefficient for line loss which was considered to be 0.9, w_2 is the weighted coefficient for generator bus voltage which was considered to be 0.1, K_D is the generator damping ration coefficient, N is the number of bus.

D. Effect of HVDC on Generator Oscillation Damping

The effect of HVDC VSC on the system generator oscillation damping ratio stability of the selected critical buses was evaluated. The HVDC VSC consists of two converter stations and a high voltage DC line connecting them. Each converter was connected at a node in the AC transmission system as shown in Figure 2 [12].

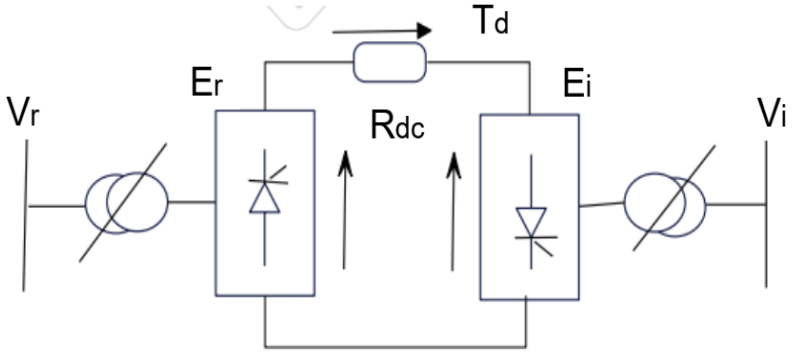

Figure 2: Single Line diagram of Transmission System with HVDC VSC

The compensator device was employed as generator control device to inject reactive power at selected severe buses where the L-VSI is outrageous during contingencies.

The converter DC link model Equations relating variables are given in Equations (9) to (12) [3, 21, 28]:

$$V_{HVDCi} = K_{ni} V_i \cos\delta - \frac{3}{\pi} X_i I_{HVDC} \quad (9)$$

$$V_{HVDCr} = K_{nr} V_r \cos\gamma - \frac{3}{\pi} X_r I_{HVDC} \tag{10}$$

$$P_{HVDCi} = V_{HVDCi} I_{HVDC} \tag{11}$$

$$P_{HVDCr} = V_{HVDCr} I_{HVDC} \tag{12}$$

The apparent power of the AC variable and the new converter voltage were calculated as in Equations (13) and (14) [19, 26]:

$$S(L) = V_{HVDC(L)} I_{HVDC} + jV_{HVDC(L)} I_{HVDC} \tan\theta(L) \tag{13}$$

$$V_{HVDC(L)} = \frac{3\sqrt{2}}{\pi} V(L) \tag{14}$$

where; V_{HVDCi} and V_{HVDCr} are converter terminal dc bus bar sending and receiving voltage, K_{ni} is the converter gain constant, V_i and V_r are sending and receiving system voltage, I_{HVDCi} is the converter current. X_i and X_r are system reactance, γ and δ are converter firing and extinction angle, $V(L)$ is the alternating voltage

Using swing equation, the HVDC voltage AC source with damping state variable is determined using Equation (15) [14, 17].

$$V_{HVDC} = \frac{-K_{nC}}{K_e}\left\{L - VSI + \frac{T_1}{T_2}\Delta\omega(t - \delta(t))\right\} \tag{15}$$

The generator excitation voltage is updated using Equation (16) [11];

$$\dot{E}'_f = \frac{K_e}{T_e} = \left(U_{ref} - U_t + V_{HVDCS}\right) - \frac{E_f}{T_e} \tag{16}$$

The electrical powers of the generator are determined using Equation (17) [4]:

$$P_{ei} = E_i^2 Y_{ii} \cos\theta_{ii} + \sum_{\substack{i=1 \\ j\neq 1}}^{N} |E_i||E_j||Y_{ij}| \cos(\theta_{ij} - \delta_i + \delta_j) + D_{HVDC} \tag{17}$$

HVDC generator stability responses are determined using Equation (18) [12, 17]

$$\frac{H\partial^2\Delta\delta}{\omega \cdot \partial t^2} + D_{HVDC}\frac{\partial}{\partial t} = \Delta P_m - \Delta P_e \tag{18}$$

The size of the controllers required for compensation is given in Equation (19):

$$S_{Value} = \frac{Q_{HVDC}}{2\pi \cdot f \cdot V_i^2} \tag{19}$$

where; ω is the generator rotor angle speed, K_e is the exciter gain constant, T_e is exciter time constant, U_{ref} is the reference bus voltage, U_t is the generator terminal voltage, V_{HVDC} is the controller control voltage, T_1 and T_2 are damping time constant, $\partial(t)$ is the damping input signal transmission delay, τ is the delay upper bound or delay margin, μ is the delay variation ratio, D_{HVDC} is the controller damping torque coefficient, K_e is exciter gain constant, f is the optimization fitness function.

Simulation for system stability response with HVDC for generator oscillation damping ratio was carried out in MATLAB R(2023a) and the flowchart is shown in Figure 3.

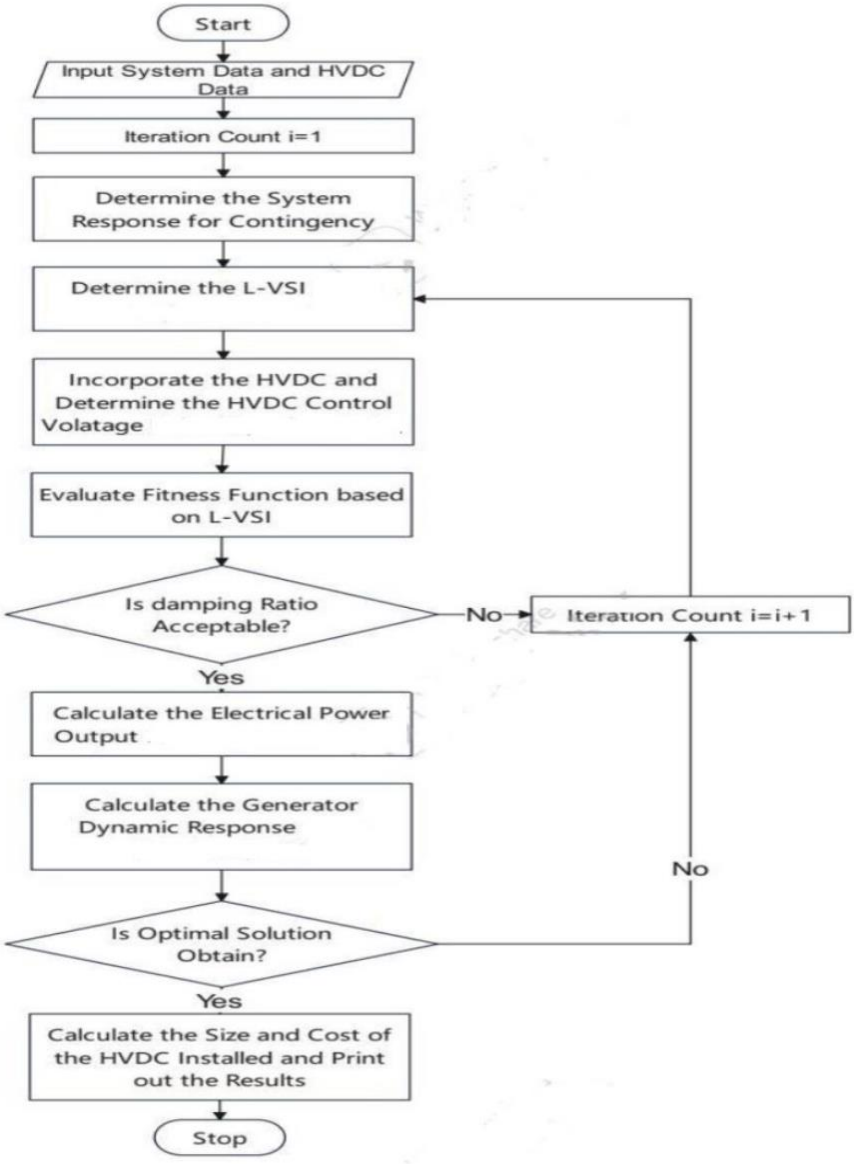

Figure 3: Flowchart of Power System Response with HVDC VSC

II. RESULTS AND DISCUSSION

In this section, the simulation results of effect of placing HVDC VSC on the stability of power system generator damping ratio at contingency on IEEE 30 bus are presented. The minimum and maximum damping ratio were set to 0.03 and 0.05 to obtain the transient stability behavior of the system generator oscillation. The line loss and change in bus voltage based on generator oscillation damping ratio were determined. In addition, the voltage working range values of the

load flow are ignored since the concern of this research is to validate the performance of the power system with respect to the generator damping ratio limit.

Figure 4 illustrated the relationship between the damping ratio and the bus number of the power system at 50% loading. It was observed that buses 5, 7, 16, 19 and 23 are the buses whose generator oscillation damping ratio were fell short of the working range with damping ratio value of 0.08, 0.06, 0.06, 0.08 and 0.08, respectively, and therefore potential buses for placement of HVDC VSC. The line loss and change in the voltage bus of these buses were 0.27, 0.06, 0.01, 0.93 and 0.17 p,u; 0.09, 0.07, 0.08, 0.09 and 0.08 p.u, respectively as illustrated in Table 1. In addition, the voltage magnitudes of these buses were reduced to 0.9310, 0.9430, 0.9329, 0.9341 and 0.9201 compared with the steady state values of 0.9360, 0.9970, 1.0150, 0.9950 and 1.0570 p.u, respectively. Figure 5 presented the results of the total power losses in the system at 50% increase in load. The total active and reactive power losses in the system were increased to453.06 MW and 328.85 MVar which is higher compared to the steady state values of 324.31 MW and 228.85 MVar, respectively.

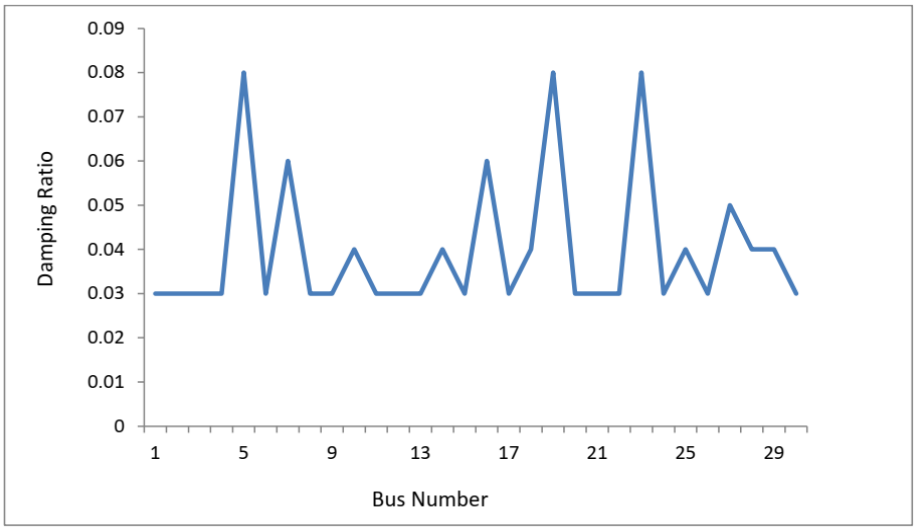

Figure 4: Damping ratio and bus number of IEEE 30-bus system at 50% loading

Table 1: Line loss and bus voltage of selected buses of IEEE 30-bus at 50%

Bus No	Voltage Magnitude (p.u)	Line Loss (p.u)	Bus Voltage (p.u)
5	0.9310	0.27	0.09
7	0.9430	0.06	0.07
16	0.9320	0.01	0.08
19	0.9341	0.93	0.09

23	0.9201	0.17	0.08

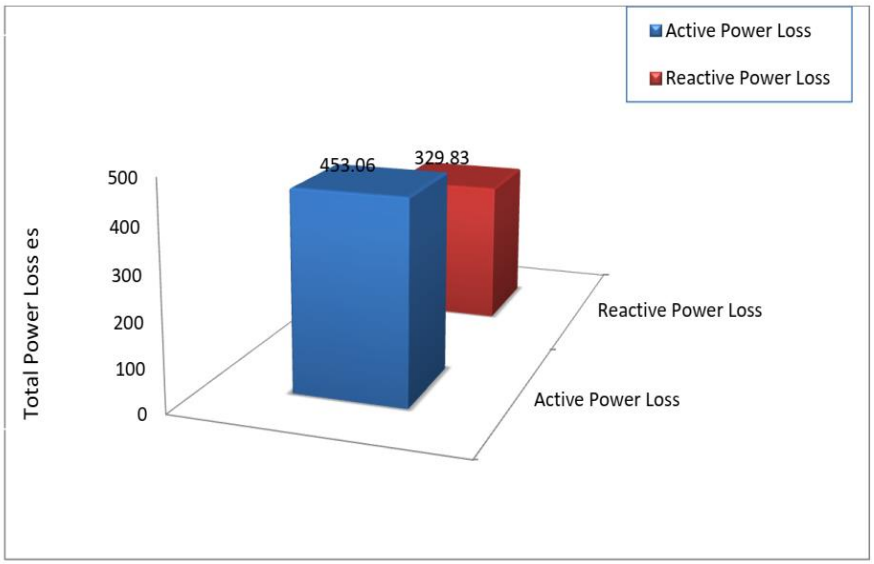

Figure 5: Total power losses of IEEE 30-bus at 50% loading

At 70% loading, the relationship between the damping ratio and the bus number of the power system is depicted in Figure 6. It was observed that buses 5, 7, 16, 19, 23 and 24 were the buses whose generator damping ratio were fell short of the working range with damping ratio value of 0.09, 0.08, 0.08, 0.07, 0.09 and 0.08, respectively. Table 2 also, displayed the results of line loss and change in the bus voltage of the selected buses with values of 0.33, 0.08, 0.02, 0.11, 0.04 and 0.24 p,u; 0.11, 0.09, 0.10, 0.08, 0.11 and 0.12 p.u, respectively. In addition, Figure 7 displayed the results of the total power losses in the system at 70% loading. The total active and reactive power losses in the system were increased to 543.66 MW and 396.90 MVar compared to the steady state values.

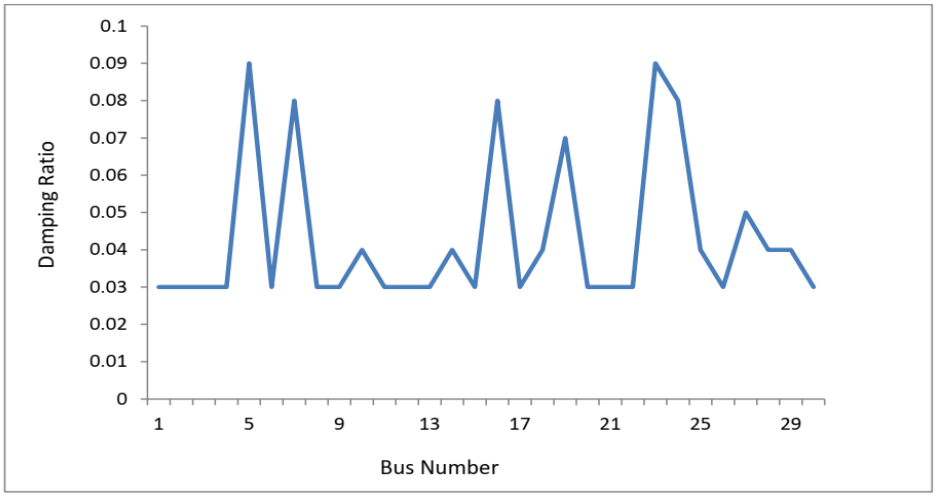

Figure 6: Damping ratio and bus number of IEEE 30-bus system at 70% loading

Table 2: Line loss and bus voltage of selected buses of IEEE 30-bus at 70%

Bus No	Voltage Magnitude (p.u)	Load Loss (p.u)	Bus Voltage (p.u)
5	0.9002	0.33	0.11
7	0.9210	0.08	0.09
16	0.9002	0.02	0.10
19	0.9041	0.11	0.08
23	0.9001	0.04	0.11
24	0.9000	0.24	0.12

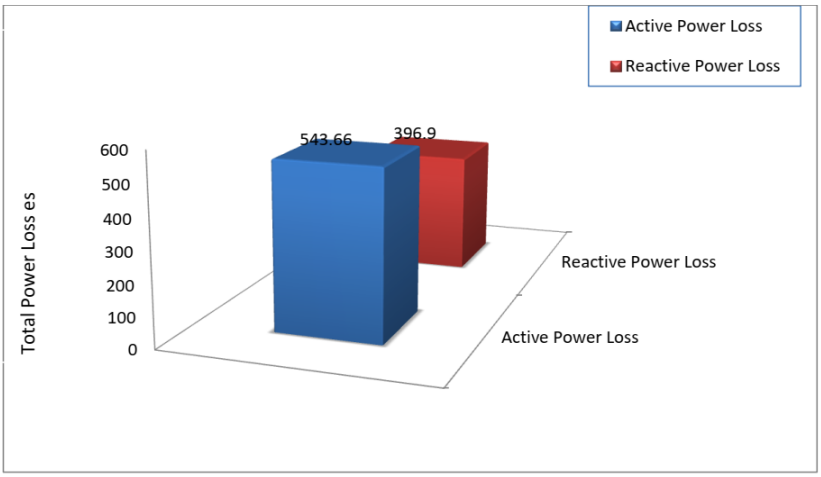

Figure 7: Total power losses of IEEE 30-bus at 70% loading

Figure 8 presented the results of the damping ratio and the bus number of the power system at 90% loading. It could be observed that buses 5, 7, 16, 19, 23, 24, 26 and 29 were the buses that fell short of the damping ratio working range with damping ratio value of 0.08, 0.08, 0.09, 0.09, 0.08, 0.09, 0.08 and 0.09, respectively, and therefore potential buses for placement of compensator devices. The line loss and change in the bus voltage of these buses were 0.39, 0.85, 0.02, 0.14, 0.26, 0.29, 0.03 and 0.01 p,u; 0.10, 0.09, 0.11, 0.10, 0.13, 0.10 and 0.13 p,u; respectively as illustrated in Table 3. In addition, Figure 9 presented the results of the total power losses in the system at 90% increase in load. The total active and reactive power losses in the system were increased to 652.05 MW and 476.3 MVar and this could result to total voltage collapse of the power system

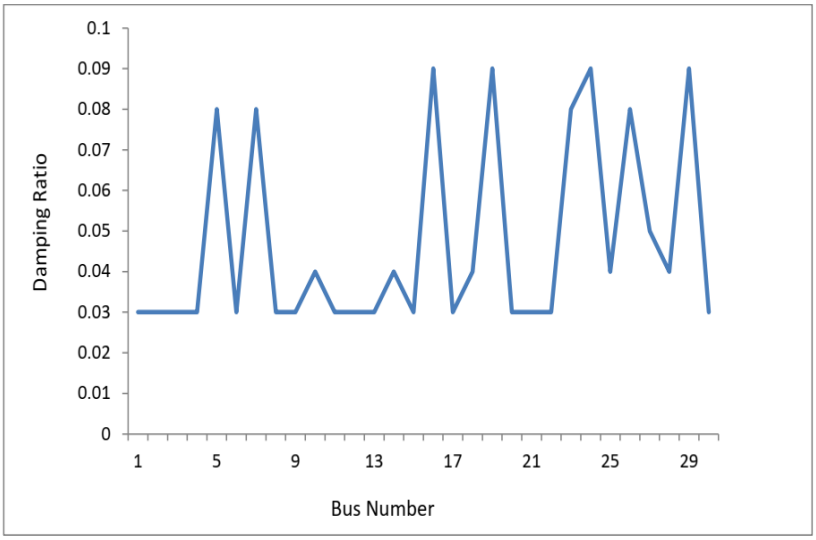

Figure 8: Damping ratio and bus number of IEEE 30-bus system at 90% loading

Table 3: Line loss and bus voltage of selected buses of IEEE 30-bus at 90%

Bus No	Voltage Magnitude (p.u)	Load Loss (p.u)	Bus Voltage (p.u)
5	0.9000	0.39	0.10
7	0.9202	0.85	0.09
16	0.9000	0.02	0.11
19	0.9200	0.14	0.10
23	0.9000	0.26	0.10
24	0.9000	0.29	0.13
26	0.9000	0.03	0.10
29	0.9000	0.01	0.13

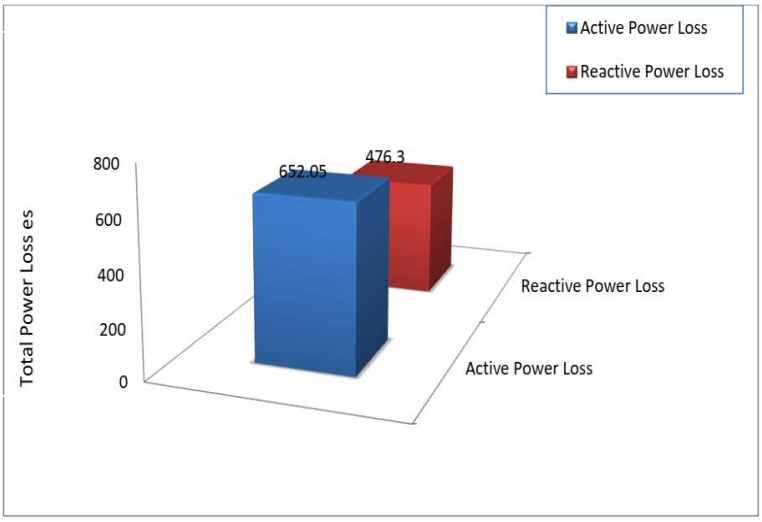

Figure 9: total power losses of IEEE 30-bus at 90% loading

Table 4 showed the results of selected buses without and with HVDC VSC reinforcement of IEEE 30-bus system at 50% loading. It was observed that an appropriate HVDC size of 400 km long, 300 MW with corresponding cost of 176.2 M$ were placed at selected optimal buses 5, 16 and 23, respectively. It was observed that the voltage magnitude and generator damping ratio of the selected buses at the contingency (5, 7, 16, 19 and 23) without HVDC were improved to 0.9500, 1.0500, 1.0105, 1.0000 and 1.0459 p.u.; 0.04, 0.04, 0.03, 0.03 and 0.04, respectively. Figure 10 presented the comparison of total active power losses of the IEEE 30-bus system without and with HVDC VSC reinforcement at 50% loading. The total active power loss in the power system was reduced to 301.92 MW compared to steady state and contingency value of 324.36 and 453.06 MW.

Table 5 presented the results of selected buses without and with HVDC VSC reinforcement of IEEE 30-bus system at 70% loading. It was observed that an appropriate HVDC size of 470, 400 and 470 km long, 350, 300 and 350 MW with corresponding cost of 201.5, 176.2 and 201.5 M$ were placed at selected optimal buses 5, 16 and 23, respectively. It was observed that the

generator damping ratio of the selected buses at the contingency (5, 7, 16, 19, 23 and 24) without HVDC were improved to 0.04, 0.03, 0.03, 0.03, 0.04 and 0.03, respectively. In addition, Figure 11 showed the comparison of total active power losses of the power system without and with HVDC VSC reinforcement at 70% loading. The total active power loss in the power system was reduced to 310.01 MW compared to the contingency value.

Table 6 showed the results of selected buses without and with HVDC VSC of IEEE 30-bus system at 90% loading. It was observed that an appropriate HVDC size of 470 km long, 350 MW with corresponding cost of 201.5 M$ were placed at selected optimal buses 5, 16 and 23, respectively. It was observed that the voltage magnitude and generator damping ratio of the selected buses at the contingency (5, 7, 16, 19 and 23) without HVDC were improve to 1.0000 p.u. each and 0.04 each, respectively. In addition, Figure 12 showed the comparison of total active power losses of the power system without and with HVDC VSC reinforcement at 90% loading. The total active power loss in the power system was reduced to 318.63 MW compared with steady state and contingency values of 324.36 and 652.05 MW.

Table 4: Effect of HVDC VSC on IEEE 30-bus system at 50% loading

	without HVDC		With HVDC				
Bus No	Voltage Magnitude (p.u)	Damping Ratio	Voltage Magnitude (p.u)	Damping Ratio	Size (MW)	Transmission Length (km)	Unit Cost (M$)
5	**0.9310**	**0.02**	**0.9500**	**0.04**	300	400	176.2
7	0.9430	0.01	1.0050	0.04	---	---	---
16	**0.9320**	**0.06**	**1.0105**	**0.03**	300	400	176.2
19	0.9341	0.01	1.0000	0.03	---	----	----
23	**0.9201**	**0.01**	**1.0450**	**0.04**	300	400	176.2

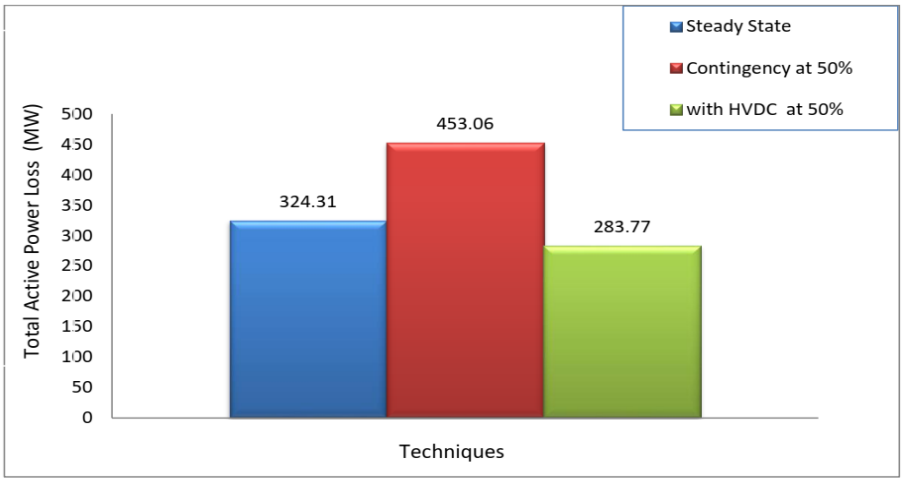

Figure 10: Comparison of total active power loss of IEEE 30-bus system at 50% loading with HVDC

Table 5: Effect of HVDC VSC on IEEE 30-bus system at 70% loading

	without HVDC		With HVDC				
Bus No	Voltage Magnitude (p.u)	Damping Ratio	Voltage Magnitude (p.u)	Damping Ratio	Size (MW)	Transmission Length (km)	Unit Cost (M$)
5	**0.9002**	**0.01**	**0.9560**	**0.04**	350	470	201.5
7	0.9210	0.01	0.9970	0.03	---	---	---
16	**0.9002**	**0.02**	**1.0150**	**0.03**	300	400	176.2
19	0.9041	0.01	0.9950	0.03	---	----	----
23	**0.9001**	**0.02**	**1.0450**	**0.04**	350	470	201.5
24	0.9000	0.03	0.9630	0.03	----	----	---

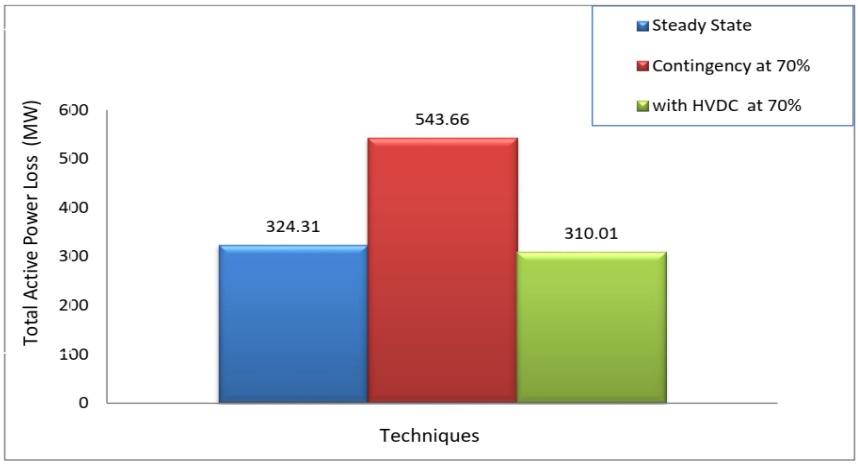

Figure 11: Comparison of total active power loss of IEEE 30-bus system at 70% loading with HVDC

Table 6: Effect of HVDC VSC on IEEE 30-Bus system at 90% loading

	without HVDC		With HVDC				
Bus No	Voltage Magnitude (p.u)	Damping Ratio	Voltage Magnitude (p.u)	Damping Ratio	Size (MW)	Transmission Length (km)	Unit Cost (M$)
5	**0.9000**	**0.01**	1.0000	0.04	350	470	201.5
7	0.9202	0.01	1.0000	0.04	---	---	---
16	**0.9000**	**0.02**	1.0000	0.04	350	470	201.5

19	0.9200	0/01	1.0000	0.04	---	----	----
23	**0.9000**	**0.02**	1.0000	0.04	350	470	201.5
24	0.9000	0.03	1.0000	0.04	----	----	---
26	0.9000	0.01	1.0000	0.04	----	----	----
29	0.9000	0.01	1.0000	0.04	----	----	----

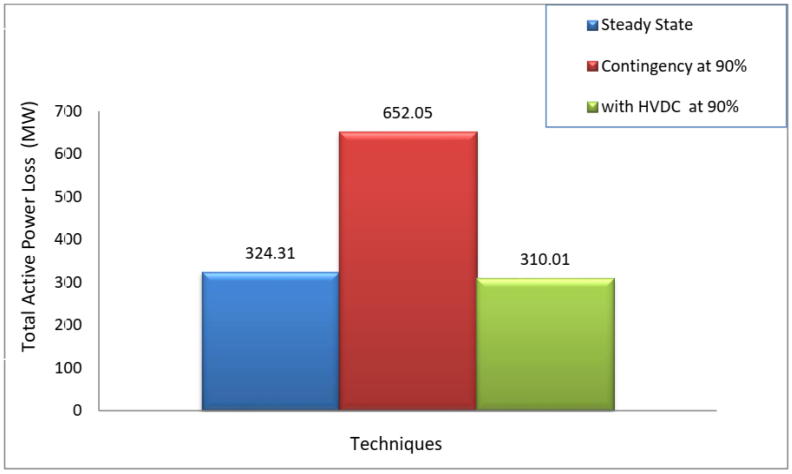

Figure 12: Comparison of total active power loss of IEEE 30-bus system at 90% loading with HVDC

III. CONCLUSION

This study has successfully presented the effect of incorporating the HVDC VSC on electric power system generator oscillation damping ration. The L-VSI was used to identify the critical buses for placement of the HVDC VSC on standard IEEE 30-bus system. The effect of placing HVDC VSC on the power system revealed that the generator oscillation damping ratio was reduced within the acceptable limit and this caused a reduction in the system active and reactive power losses, increase in customer energy growth and improvement in voltage magnitude of the power system. Thus, it can be concluded that the effect of placing HVDC on the power system improved the system generator oscillation stability and has positive impact (stability) on electric power system

REFERENCES

[1] Adebayo, I. G. and Sun, Y. (2022). New approaches for the identification of influential and critical nodes in an electric grid. Archives of Electrical Engineering, **71**(3), pp. 671 –686.

[2] Adebayo, I. G., Jimoh, A. A., Yusuff, A. A. and Sun, Y. (2018b). Alternative method for the identification of critical nodes leading to voltage instability in a power system. *African Journal of Science, Technology, Innovation and Development*, 1-2, doi: 10.1080/20421338.2018.1461967

[3] Adebayo, I. G., Jimoh, A. A. and Yusuff, A.A. (2016). Voltage stability assessment and identification of important nodes in power transmission network through network response structural characteristics. *The Institution of Engineering and Technology Generation, Transmission and Distribution*, **11** (6): 1398-1408.

[4] Al-Tameemi, Z. H., Enawi, H. H., Al-Anbar, K. M. and Almukhtar, H. M. (2018). Transient stability improvement of the power systems. *Indonesian Journal of Electrical Engineering and Computer Science*, **12** (3): 916~923.

[5] Amroune, M., Bouktir, T. and Musirin, I. (2019). Power system voltage instability risk mitigation via emergency demand response-based whale optimization algorithm. *Protection and Control of Modern Power Systems*, **4** (25): 1-14.

[6] Anwar, N., Hanif, A., Khan, H. F. and Ullah, M. F. (2020). Transient stability analysis of the power bus system under multiple contingencies. *Engineering, Technology and Applied Science Research*, **10**(4): 5925-5932.

[7] Anwar, N., Hanif, A., Khan, H. F., Ullah, M. F. and Ahmed, W. (2019). Analysis of transient stability of IEEE 9-bus system under multiple contingencies. *International Journal of Electrical and Power Engineering*, **13** (2) 19-29.

[8] Asplund, G. (2010). Application of HVDC light to power system enhancement, *IEEE Winter Meeting, Singapore* , Pp. 1-6.

[9] Chodura, P., Gibescu, M., Kling, W. L. and Graaff, R. A. (2023). Investigation of the impact of embedded VSC-HVDC active and reactive power control on power system stability. *IEEE Explore, Tshwane University of Technology*., 1-6.

[10] Ishtaiwi, A. (2017). An overview of HVDC applications: a study on medium voltage distribution networks. *B.sc Project Submitted to Department of Energy Engineering, School of Natural Resources Engineering and Management, German Jordanian University:* 1-47.

[11] Ismai, B., Wahab, N. A.,Othman, M. L., Radzi, M. A., Vijayakumar, K. N., Rahmat, M. K. and Matnaain, M. N. (2022). New line voltage stability index for voltage stability assessment in power system: the comparative studies. *IEEE Access, Digital Object Identifier* 1-10, 10.1109/ACCESS.2022.2.

[12] Kadiman, S., Basuki, A. and Arena, M. (2015). The dynamic of synchronous generator under unbalanced steady state operation: a case of virtual generator laboratory. *International Journal of Electrical and Computer Engineering*, **5** (6): 1292-1303.

[13] Kalunta, F. and Ngwu, O. (2022). Optimal location of VSC-HVDC system in Nigerian 330kV power network using a short circuit voltage violation index and line loss Technique. *International Transaction of Electrical and Computer Engineers System*, **7** (1): 1-10.

[14] Kamel, M., Karrar, A. and Eltom, A. (2017). Development and application of a new voltage stability index for on-line monitoring and shedding. *IEEE Transactions on Power Systems*, 1-7, DOI 10.1109/TPWRS.2017.2722984,

[15] Kieran, P., Alvin, D., Sorin, D. and Horia, A. (2019). A study on the implementation of HVDC for power system interconnection. *IEEE Journal;* 1-6, 1978-1-7281-2906-8/19.

[16] Kumar, A. and Hussain, D. M. (2018). High voltage direct current transmission system: a review paper. Gyancity *Journal of Engineering and Technology*, **4** (2): 1-10,

[17] Kumar, A. S. (2010). FACTS and HVDC technologies for the development and enhancement of future power Systems. *International Journal of Computer Communication and Information System*, **2** (1): 241-247.

[18] Moger, T. and Dhadbanjan, T. (2015). A novel index for identification of weak nodes for reactive compensation to improve voltage stability. *The Institution of Engineering and Technology Generation, Transmission and Distribution*. **9** (14): 1826–1834.

[19] Patel, P. R., Modi, T. P. and Anil S. (2013). The role of FACTS and HVDC in development of an efficient electrical power transmission system in India-prospects and challenges. *International Journal for Scientific Research and Development*, **1** (10): 2085-2093.

[20] Pinares, G. and Bongiorno, M. (2016). Modeling and analysis of VSC-based HVDC systems for DC network stability studies. *IEEE Transactions on Power Delivery*, **31** (2): 851-856.

[21] Rao, J. S. and Amarnath, J, (2014). Enhancement of transient stability in a deregulated power system using FACTS devices. *Global Journal of Researches in Engineering: Electrical and Electronics Engineering*, **14** (6): 1-17.

[22] Raouf, A. A., Kamal, S. E. and Mehanna, M. A. (2016). Impact of HVDC system on power system stability. *International Journal of Scientific and Engineering Research*, **7** (6): 1157-1163,

[23] Sanni, S.O. (2014). Assessment of transient stability enhancement capability of unified power flow controller in a multi-machine power system. *A Thesis submitted to the School of Postgraduate Studies, Ahmadu Bello University, Zaria*. 1.30.

[24] Selwa, F., Djamel, L. and Imen, L. (2015). The transient stability study of a synchronous generator based on the rotor angle stability. *International Journal of Electrical and Computer Engineering*, **5** (6):1319~1327.

[25] Shafqat, M. and Pankhuri K. (2010). Implementation and application of HVDC in context to new electric industry, 1-7, https://www.researchgate.net/publication/319877202

[26] Shukla, H. S., Thakkar, V., Trivedi, D. S., Mishra, P. R., Joshi, A. R. and Shukla, B. S. (2020). Transient stability analysis of synchronous generator in power system. *International Research Journal of Engineering and Technology*, **7** (6): 589-593.

[27] Srikanth, P., Rajendra, O., Yesuraj, A., Tilak, M. and Raja, K. (2013). Load flow analysis of IEEE14-bus system using MATLAB. *International Journal of Engineering Research and Technology*, **2** (5): 149-155.

[28] Sugiarto, D. Hadi, S. P., Tumiran, F and Wijaya, D. (2013). Teaching the large synchronous generator dynamic model under unbalanced steady-state operation. *Conference Paper*, 1-6, www.researchgate.net/publication/: doi:10.1109/IC.2013.66777.

[29] Tibin, J., Loo, C. U., Li, G., Jun, L., Oluwole, D. A., Rahman, M. H. and Ian, C.. (2021). Impact of grid strength on HVDC connection requirements. *IEEE Journal;* 586-591, 978-1-7281-6344-4/21.

[30] Yousuf, S. M. and Subramaniyan, M. S. (2013). HVDC and Facts in power system. *International Journal of Science and Research,* **29** 12): 133-138.